Use of Curcumin as Sensitizer with ZnO nanoparticles for Visible Light Photocatalytic Degradation of Methylene Blue

Hinane Baleh[1], Salah Bassaid[1], Abdelkader Dehbi[1,*], Abderrahmen Benaouda[1], Asmaa Bouazza[1], Ali Alsalme[2], Barbara Bonelli[3] and Massimo Messori[3]

[1] *Engineering Physics Laboratory, University of Tiaret, Tiaret, 14000 Algeria.*

[2] *Department of Chemistry, College of Science, King Saud University, Riyadh 11451, Saudi Arabia.*

[3] *Department of Applied Science and Technology (DISAT), Politecnico di Torino, Corso Duca degli Abruzzi 24, 10129 Torino, Italy*

*Corresponding author: *Dehbi Abdelkader, Email:* abddehbi@gmail.com

Abstract

This work aims to examine the application of ZnO/Curcumin nanocomposite materials, in which curcumin (natural dye) is used as a photosensitizer in the photocatalytic degradation of methylene blue (MB) under visible light irradiation. The ZnO/x%Curcumin nanocomposite materials (with x = 3, 5, 7, 10 and 20) are prepared by the wet impregnation method. These nanocomposite materials are characterized using various techniques; including Fourier transform infrared (FT-IR) spectroscopy, X-ray diffraction (XRD), ultraviolet-visible (UV-Vis.) spectroscopy and scanning electron microscopy (SEM). Optimal MB degradation of ~99% was obtained with a concentration of 0.5 g.L^{-1} of 5% curcumin/ZnO nanocomposite catalyst material, at natural pH and initial MB concentration of 10 mg.L^{-1} for 90 min exposure to visible light irradiation. The kinetic indicates that the Langmuir-Hinshelwood (L-H) model is well adapted to the experimental data. A pseudo-first-order kinetics were obtained with a rate constant (k) and half-life time ($t_{1/2}$) of 0.0423 min^{-1} and 16 min, respectively. The significant improvement in the photocatalytic properties of ZnO under visible light irradiation induced by the addition of curcumin as a photosensitizer could be due to the increase in the concentration of reactive radical species in the solution, such as superoxide ($O_2^{\bullet -}$) and hydroxyles ($OH^{\bullet}$).

Keywords: Curcumin, Zinc Oxide, Methylene Blue, Photocatalysis, Photosensitizer.

1. Introduction

Water depollution poses a serious problem for the scientific community due to uncontrolled discharge into the environment of water containing various recalcitrant organic dyes from the textile, cosmetic and food industries, leading to deterioration of naturel water bodies because of their high toxicity [1-3]. Conventional physicochemical and biological methods applied for

water depollution were based on the use of ion exchange resins [4], activated carbon [5], solvent extraction [6] and reverse osmosis [7]. Experience has shown that all these processes are inefficient in removing these recalcitrant organic dyes. Hence, the necessity to look for better alternatives. In this context, heterogeneous photocatalysis with semiconductor materials represents nowadays an emerging solution to pollution problems and shows its potential for achieving efficient degradation of these compounds. Titanium dioxide, TiO_2, especially the anatase form, is considered an excellent semiconductor-photocatalyst capable of mineralizing a wide range of organic pollutants into CO_2 and H_2O. TiO_2 is the most studied material for such applications due to its high oxidizing capacity, less toxicity and low cost [8]. Alternatively, ZnO can be considered as the second oxide used in photocatalysis [9], with physicochemical properties comparable to those of TiO_2. At high redox potential, the ZnO semiconductor has a bandgap energy (E_g = 3.20 eV) [10]. In addition, it has a good piezoelectric characteristics, chemical stability and biocompatibility [11, 12]. One of the limiting factors that control the efficiency of photocatalysts is the very rapid recombination of photogenerated electron-hole pairs ($e^- - h^+$) within the semiconductor particles. Currently, numerous studies are being conducted to limit this phenomenon. Among the proposed solutions, the following are mentioned: coupling with another appropriate semiconductor [13]; chemical doping with atoms such as sulfur, chloride [14], and transition metals (Co and Cu) [15]; coupling with a sacrificial solid agent, such as calcium oxalate [16] and sensitization with natural dyes- [17]. In recent years, natural dye-sensitization has become a promising technique in the field of removal of pollutants from real wastewater because these natural dyes are cost-effective, non-toxic, abundant and environment-friendly, which can be easily extracted from natural sources such as bloom petals, leaves and bark of the plants [18, 19]. Some existing studies already confirm that the activity of certain semiconductors, such as TiO_2, can be effectively improved by combining it with a sensitizer, such as curcumin (a natural substance) [18]. Curcumin was chosen here because it is non-toxic, anti-inflammatory, anti-cancer, available, easy to extract, and it can establish better anchoring due to the interaction of hydroxyl groups with ZnO.

In a recent study, our team carried out the photocatalytic degradation of Methylene Blue (MB) in the presence of the TiO_2/curcumin nanocomposite material, in suspension mode [20] and in dynamic mode, where the TiO_2/Curcumin nanocomposite material was deposited on a cellulosic paper substrate [21]. The obtained photocatalytic activity results showed significant degradation of MB. Indeed, a degradation percentage of 63% was obtained for the TiO2/5%Curcumin material in suspension mode and a degradation percentage of 85% was obtained, in dynamic mode, for a mass of 14 mg of the TiO_2/5%Curcumin material deposited on the cellulose paper.

This work concerns, in the first part, the development of ZnO/x% curcumin nanocomposite materials (with x =3, 5, 7, 10 and 20), where curcumin is incorporated by the wet impregnation method on the surface of ZnO nanoparticles, to improve its photocatalytic performance due to the absorption characteristics of curcumin in the visible region. The physicochemical characterization of ZnO/x% curcumin (with x =3, 5, 7, 10 and 20) nanocomposite materials was investigated using different analysis techniques. In the second part, the photocatalytic properties of the samples were tested against MB as a model recalcitrant compound under visible light.

2. Materials and methods

2.1. Reactants

Zinc acetate di-hydrate ($Zn(CH_3COO)_2 \cdot 2H_2O$) was purchased from Sigma-Aldrich, isopropanol (C_3H_8O, 99.5%) was purchased from Sigma-Aldrich, Curcumin ($C_{21}H_{20}O_8$, 99%) and methylene blue dye ($C_{16}H_{18}N_3ClS$) from Biochem; ethanol (C_2H_5OH, 96%) and sodium hydroxide (NaOH) from Sialchim. All chemicals used to prepare ZnO/x% curcumin (with x = 3, 5, 7, 10, 20) nanocomposites were used without further purification.

2.2. Synthesis of nanoparticles of ZnO

To synthesize the zinc oxide (ZnO) powder, zinc acetate di-hydrate ($Zn(CH_3COO)_2 \cdot 2H_2O$) and sodium hydroxide (NaOH) were used as precursors and distilled water (DW) was used as solvent. A controlled amount of $Zn(CH_3COO)_2 \cdot 2H_2O$ was dissolved in 75 ml distilled water under constant stirring for 15 min at 60°C. An aqueous solution of NaOH was added dropwise for 10 min to the reaction mixture under constant stirring until the pH of the solution reached to 8. During this process, a white precipitate formed. After 4 hours, the reaction mixture was filtered to get the precipitate out and washed several times with both distilled water and ethanol. Finally, the obtained powders were calcined at 500°C for 4 hours in a furnace to get a nanocrystalline ZnO white powder [22].

2.3. Preparation of ZnO/x% Curcumin nanocomposite materials (with x =3, 5, 7, 10 and 20)

ZnO/x% curcumin nanocomposite materials (with x = 3, 5, 7, 10, 20) were prepared by wet impregnation method, which consists of anchoring easily the curcumin onto the ZnO-particles surface by adding an appropriate amount of curcumin dissolved in a 50 ml of isopropanol to 1 gram of prepared ZnO to obtain a sample with x% by weight of curcumin at the end. The

obtained mixture was then constantly stirred at room temperature for 3 hours. After this stirring time, the solution was filtered under vacuum and dried at 100°C for 5 hours [18].

2.4. Characterization methods

The FT-IR spectra of different samples of ZnO/x%curcumin nanocomposite (with x = 3, 5, 7, 10, 20) were recorded in the 400-4000 cm^{-1} range using a SHIMADZU spectrometer with a resolution of 4 cm^{-1}. The samples were carefully ground and mixed with dry KBr in a proportion of 1%, then crushed and compacted into pellets.

In order to examine the absorbance of ZnO/x%curcumin nanocomposites (with x = 3, 5, 7, 10, 20) in the UV-visible range, the powders of these materials were finely divided and well dispersed in ethanol under agitation in an ultrasonic bath for 20 min, then analyzed in the 300-600 nm range. The UV-visible spectrophotometer used was a SHIMADZU 1650 PC dual beam device.

The structure of the ZnO/x%curcumin nanocomposites powders (with x = 3, 5, 7, 10, 20) was characterized by X-ray diffraction (XRD) using the RigaKu miniflex 600 instrument with an anticathode of Cu-K_α ($\lambda = 1.54$ Å). The step size was 0.02° while the scan speed was 4°/min. The crystallite size (*Dc*) of the particles was calculated by using the following Debye- Scherrer equation (Eq. 1) [23].

$$Dc = \frac{K\lambda}{\beta cos\theta} \quad (1)$$

Where K is Scherrer constant (0.90), 2θ is the angle of diffraction λ is the X-ray wavelength and β is the full width at half-maximum of the diffraction peak.

Scanning Electron Microscopy (SEM) images were taken using a Carl Zeiss AG - SUPRA 40 (Resolution 1.3 nm at 15 kV, 2.1 nm at 1 kV, and 5.0 nm at 0.2 kV). Samples were prepared by lightly pressing each powdered material into the cavity of the sample holder. Each sample was then metalized with gold to establish an electrical contact.

2.5. Photocatalytic activity experiments

Photocatalytic degradation experiments of MB were performed in a double-walled reactor. This reactor was irradiated by two tungsten lamps (visible light) with a power of 75 W each, located next to the reactor in a fixed position, and the irradiation time was 90 min. The operating temperature was fixed during the experiment at 25°C by the circulation of water. Pure Curcumin and ZnO/x%curcumin nanocomposite (with x = 0, 3, 5, 7, 10 and 20) were dispersed through stirring in a volume of 100 ml of MB aqueous solution ([MB] = 10 mg L^{-1}). The suspension was homogenized by a magnetic stirrer and remained in contact with air. Before each irradiation, the mixtures were sonicated for 5 min to disperse the catalyst, and the suspensions were kept in the dark for 60 min to reach the adsorption equilibrium conditions. During the photocatalytic test, aliquots of 3 mL were taken out at regular time intervals, filtered, and analyzed by UV-vis. 1650PC spectrophotometer (λ_{max}= 664 nm).

3. Results and discussion

3.1. Characterization results of ZnO/x%Curcumin (with x = 3, 5, 7, 10 and 20)

3.1.1. Fourier transform infrared (FT-IR) analysis

Figure 1 shows the FT-IR spectra of ZnO/x%Curcumin nanocomposite materials (with x = 3, 5, 7, 10 and 20), compared with that of pure Curcumin and pure ZnO. According to the figure, the characteristic curcumin peaks, summarized in Table 1, are in good agreement with the literature [24 - 31].

Regarding the spectra of the ZnO/x%curcumin nanocomposite materials (with x = 3, 5, 7, 10 and 20), it is seen that the characteristic peaks of pure ZnO can be identified. The main observations, drawn from these spectra, can be given as follows:

- A broad vibration band located at 400 cm^{-1} (highlighted in red in the figure) corresponds to the Zn-O bond vibration.
- All the characteristic bands of ZnO appear in the ZnO/x%curcumin nanocomposites and decrease in intensity as the percentage of the curcumin increases.
- Broad peaks at 3434 cm^{-1} and at 1330 cm^{-1} indicate the presence of atmospheric humidity [32, 33].

Additionally, it is clearly observed that starting from a curcumin percentage of 10%, the characteristic peaks of curcumin become apparent in the FT-IR spectra of the nanocomposite materials, indicating the formation of a separate phase of curcumin in the nanocomposite. For ZnO/x%curcumin nanocomposites with a curcumin percentage below 10%, no curcumin peak

is observed in their spectra. Based on this result, it can be concluded that the addition of curcumin does not affect the ZnO structure in the ZnO/x%Curcumin nanocomposites (with x =3, 5 and 7). This may be due to the low quantity of curcumin added compared to that of ZnO into the nanocomposite, which suggests that the structure of nanocomposite is imposed by that of ZnO.

3.1.2. X-ray diffraction analysis (XRD)

Figure 2 reports the XRD patterns of the ZnO/x%Curcumin nanocomposite materials (with x = 3, 5, 7, 10 and 20), as compared to those of ZnO and Curcumin alone.

The XRD results show that curcumin was in a highly crystallized state and exhibited several sharp diffraction peaks at 2θ from 9° to 30° (9.02, 12.42, 14.74, 17.38, 18.30, 21.34, 23.44, 24.84, 27.60 and 29.22°), which is in good agreement with previous studies [34]. In the case of ZnO/x%Curcumin nanocomposites, the XRD patterns show that the most intense peak of curcumin (2θ = 17.38 °) appears only in the ZnO/20%curcumin nanocomposites. For curcumin percentages below 20%, this peak is absent, in agreement with FT-IR spectroscopy. As for the ZnO peaks, they all appear in all the ZnO/x%curcumin nanocomposites (with x =3, 5, 7, 10 and 20), showing that the incorporation of curcumin into the nanocomposites does not affects the structural stability of ZnO.

The average nanoparticles size for Curcumin-doped ZnO varies little with the curcumin ratio, which implies that the presence of curcumin did not affect the structure of ZnO and no new phase was formed. Indeed, the crystallite size values obtained (Table 2) are between 15.25 nm and 15.85 for the ZnO/x% curcumin nanocomposite materials (with x = 5, 7, 10 and 20), with the exception of that of ZnO/3% curcumin where a value of 12.44 nm is obtained.

3.1.3. UV-visible optic analysis

The UV-Visible absorption spectra of ZnO, curcumin and ZnO/x%curcumin nanocomposites (with x = 3, 5, 7, 10 and 20) are shown in Figure 3. The spectrum of ZnO shows some wide bands: many energetically close transitions are indeed responsible for these absorptions, since the vibrational and rotational substructures, within the same electronic level, can lead to energy transition of the same order of magnitude, starting and ending at the same electronic levels, but involving different vibrational and rotational levels. Different electromagnetic radiation of slightly different wavelengths then leads to different energetically very close transitions and thus to absorption bands. In the case of curcumin (an organic molecule), the absorption band is also wide, the electronic levels affected by transitions in the UV-visible correspond roughly to

σ and π bonds and to their binding, anti-binding and non-binding character. Schematically, the relative order of the electronic levels is presented in figure S1 [35]. As for the nanocomposites, a maximum wavelength (λ_{max}) shift from 390 nm to 450 nm and an increase in the absorption band with an increasing ratio of curcumin in the nanocomposite are recorded. This may be due to the presence of multiple bonds and non-binding doublets, which generally allow good absorption in the visible range. Furthermore, the conjugation of the π system of curcumin leads to a tightening of π and π* levels (Figure S2).

3.1.4 Microstructural analysis (SEM)

The Scanning Electron Microscopy (SEM) images of ZnO, Curcumin and ZnO/x%curcumin system (with x = 5, 10 and 20) are shown in Figure 4a-e. Figure 4-b shows the SEM image of ZnO nanobelts at 30,000x magnification. The product consists of a well-defined shape and has a round morphology. The diameter of nanobelts is on the order of 290 nm and the majority of nanobelts are around 1 µm in length. At 10,000x magnification, the curcumin morphology (Fig. 4a) is most evident as a rough surface on which a broad distribution of curcumin chunks of different sizes heterogeneously distributed forming an indefinite shape [36]. The SEM images of the mixtures of the ZnO/x% curcumin system produced, as illustrated in Figures 4c-e. It is interesting to note the existence of various spherical particles with nanometric dimensions for curcumin-doped zinc oxide. However, the existence of curcumin is associated with an even better distribution of particles over the entire surface of the matrix. This shows a great homogeneity of the layers of samples.

3.2. Photocatalytic activity

3.2.1. The real nature of the photocatalytic process

As mentioned in the literature, the principle of photocatalysis is based on the excitation of a semiconductor by light (UV or Visible). Under the action of photons, the semiconductor photocatalyst produces powerful oxidizing free radicals, allowing the degradation of the compounds adsorbed on its surface. The semiconductor converts photon energy into chemical energy by redox reaction. This causes activation of the semiconductor sites and molecular degradation of the compounds present. The degradation process then consists of a succession of radical oxidations, initiated by strong oxidants such as $OH^{\cdot}$ radicals, which are directly generated by the water molecules adsorbed on the active sites of the catalyst [37]. In this context, tests were carried out for two different conditions:

- Methylene Blue (MB) alone under visible irradiation in the absence of the ZnO/5%curcumin catalyst (photolysis),

- Methylene Blue (MB) under visible irradiation in the presence of ZnO/5%curcumin catalyst (photocatalysis).

Figure 5 gives the variation of the normalized concentration, C/C_0, of MB as a function of the irradiation time.

As can be seen in this figure, in the case of the test under visible irradiation without the catalyst (photolysis), no degradation of the MB dye is observed during the 60 minutes of irradiation. In the second test (photocatalysis), that is to say, when the catalyst is dispersed in the MB solution, which is exposed to visible light, the MB concentration decreases rapidly. Approximately 95% of the MB dye is removed during the 60 minutes of irradiation time. This indicates that the system works well in the pure photocatalytic regime.

3.2.2. Evaluation of the photocatalytic activity of ZnO/x%Curcumin (with x = 0, 3, 5, 7, 10 and 20)

Figure 6 gives the relative concentration of MB, C/C_0, as a function of time under visible irradiation. It appears from this Figure that the photodecomposition of MB consists of an adsorption of the pollutant on the active sites of the catalyst materials, followed by photochemical degradation. During the test in the presence of pure curcumin, a degradation percentage of approximately 20% is reached after 90 min, thus showing its low photocatalytic activity. As for pure ZnO, a degradation percentage of 30% is reached after 90 min under visible irradiation. This can be explained as follows: In the visible region ($\lambda > 400$ nm), ZnO is inactive; this is due to its large band gap. Indeed, the band gap of ZnO is 3.2 eV, it corresponds to the UV region of the electromagnetic radiation of ZnO. The degradation of MB should be explained by the sensitization of the dye by visible light photons. To summarize, when the dye is excited by visible light there is a major formation of the excited state Methylene Blue ($^{+}\boldsymbol{MB}^{*}$) (Equation (2)), which can act as a single-electron transfer (SET) to give a Methylene Blue radical ($MB^{\cdot}$) (Equation (3)) [38]. Then, an electron can be injected from the excited state of the dye adsorbed onto the conduction band of ZnO (equation (4)), and the ejected electron can be scavenged by molecular oxygen to generate the superoxide radical species (Eq. (5)), which can then form other oxidative intermediate species ($OH^{\cdot}$, $HOO^{\cdot}$ ...).

$$\boldsymbol{MB}^{+} + \boldsymbol{h\nu} \rightarrow {}^{+}\boldsymbol{MB}^{*} \quad (2)$$

$$^{+}MB^{*} \rightarrow MB^{\cdot} \quad (3)$$

$$MB^{\cdot} + ZnO \rightarrow MB^{\cdot +} + ZnO\,(e^{-}) \quad (4)$$

$$ZnO\,(e^{-}) + O_2 \rightarrow ZnO + O_2^{\cdot -} \quad (5)$$

The results of the MB photocatalytic degradation in the presence of ZnO/x% Curcumin nanocomposites (with x = 3, 5, 7, 10 and 20) show better degradation of MB from 3% in curcumin. A maximum photocatalytic degradation of 99% is observed for a nanocomposite with 5% in curcumin. Beyond this value, from 7% in curcumin, a decline in photocatalytic activity is observed.

3.2.3. Kinetic of MB photocatalytic degradation

From the results of MB photocatalytic degradation in the presence of ZnO/x% Curcumin nanocomposite materials with x = 3, 5, 7, 10 and 20 (Figure S3 (B)), the rate constants, k, can be obtained from the non-linear least squares fitting to the untransformed original equation (Eq. 6) [39].

$$C = Ae^{(-kt)} + E \qquad (6)$$

A is the amplitude, k is the pseudo-first order rate constant, E is the end point and t is the reaction time.

However, it is worthwhile to outline that for the pur ZnO and pur Curcumin (Figure S3 (A)), the rate constants, k, are estimated from the zero-order model (Eq. 7).

$$C = -kt + C_0 \qquad (7)$$

The half-life times ($t_{1/2}$) can be evaluated by the following equations (Eq. 8 and Eq. 9):

Zero-order: $t_{1/2} = \frac{C_0}{2k}$ (8)

First-order: $t_{1/2} = \frac{Ln2}{k}$ (9)

The values of the rate constants (k), half-life times ($t_{1/2}$), standard deviation and correlation coefficients (R^2) are listed in Table 3. The considerable values of R^2 reflect a good fitting between the experimental results and the proposed fitting method.

The evolution of the found values of k and $t_{1/2}$ revealed a significant and favorable effect of the combination of curcumin with ZnO for MB photocatalytic deghradation under visible light. The values of the rate constant (k) and half-life time ($t_{1/2}$) of the ZnO/5% curcumin nanocomposite material show good photocatalytic activity, and they are equal to 0.0423 min^{-1} and 16 min, respectively, which will be the subject of the study of the effect of some physicochemical parameters on photocatalytic degradation.

3.3 Effect of some physicochemical parameters on photocatalytic degradation

3.3.1. Effect of stirring

Figure 7 gives the results of the study of the effect of stirring on the rate of MB photocatalytic degradation. Table 4 gives the rate constants (k), half-life times ($t_{1/2}$), standard deviation and correlation coefficients (R^2) for the MB photocatalytic degradation in the presence of the ZnO/5%Curcumin nanocomposite material with and without stirring.

The results obtained show that the MB degradation rate with stirring is 19 times higher than that without stirring. This can be attributed to: (i) stirring of the solution ensures contact between the catalyst and the dye, (ii) when the solution is stirred, the catalyst particles are better exposed to light, while when the solution is not stirred, only the upper hemisphere is exposed to light. These results are in good agreement with those obtained in the literature [18].

3.3.2. Effect of oxygenation (with air)

It is well known in the literature that oxygenation (with air) of the solution is of primary importance regarding the photocatalytic degradation of organic molecules [40]. For this reason, a photocatalytic degradation test of the MB in the presence of the ZnO/5%Curcumin nanocomposite material without O_2 (air) was carried out. The results obtained are presented in Figure 8. Table 4 gives the rate constants ($\boldsymbol{k}$), half-life times ($\boldsymbol{t_{1/2}}$) and correlation coefficients ($\boldsymbol{R^2}$) for photocatalytic degradation of MB in the presence of the ZnO/5% curcumin material under O_2 (air) and without O_2 (air).

As we can see in Figure 8, the presence of oxygen (air) in the heterogeneous medium (catalyst/light) accelerates the photocatalytic degradation of the dye (MB). Indeed, the rate of disappearance of the MB, in the case of the test under oxygen (air), is multiplied by a factor of approximately 3 compared to that of the test without oxygen (air). This acceleration may be due to the inhibition of charge recombination (e^-/h^+), which is a factor limiting the efficiency of photocatalytic degradation. The presence of oxygen promotes the separation of charges, and consequently, the production of more $O_2^{\bullet -}$ and $OH^\bullet$ radicals in the medium, thus allowing the degradation of the compounds adsorbed on the surface of the catalyst [41]. Eq. 10 gives the equation for the photocatalytic degradation reaction in the presence of oxygen:

$$OH^\bullet + \text{Pollutants} + O_2 \rightarrow CO_2 + H_2O + \text{intermediate products} \quad (10)$$

3.4. Photocatalytic mechanism under Visible light irradiation

The photocatalytic degradation mechanism under visible irradiation can be explained as follows: the considerable improvement in photocatalytic performance comes down to the junction established between the Curcumin and the ZnO oxide. Indeed, these two materials

combine closely with each other and form an interface. In the ZnO/ curcumin nanocomposites, the sensitized Curcumin absorbs photons under visible light and thus excites electrons from the HOMO (Highest Occupied Molecular Orbital) level to LUMO (Lowest Unoccupied Molecular Orbital) level of the excited singlet state of curcumin. At the same time as already seen in paragraph 3.2.2, MB (a dye-sentitizing agent) also absorbs the photon of visible light and forms an excited state ($^{+}MB^{*}$). Therefore, the excited electrons from curcumin as well as MB are ttransferredinto the conduction band (CB) of ZnO while the valence band (VB) of ZnO remains intact under visible light irradiation. These electrons react with oxygen to produce superoxide radical anion ($O_2^{\cdot -}$). The superoxide radical anion further produces hydroxyl radical ($OH^{\cdot}$) or reacts with a proton to form hydroperoxyl radical ($HOO^{\cdot}$) (Eqs. (11)-(14)) [42, 43].

$$O_2^{\cdot -} + H^+ \rightarrow HOO^{\cdot} \quad (11)$$

$$O_2^{\cdot -} + H_2O \rightarrow OH^- + H_2O^{\cdot} \quad (12)$$

$$2H_2O^{\cdot} + H_2O \rightarrow H_2O_2 + OH^{\cdot} \quad (13)$$

$$H_2O_2 \rightarrow 2OH^{\cdot} \quad (14)$$

Thus, the recombination process of the electron-hole charge pairs (e^- - h^+) is inhibited. Consequently, a significant improvement in the photocatalytic degradation of the pollutant on the ZnO/curcumin nanocomposites is observed. By this interpretation, the role played by Curcumin can be illustrated by the injection of electrons in the CB of ZnO under visible light and the possibility of the formation of extremely reactive radicals, like $O_2^{\cdot -}$, $OH^{\cdot}$ and $HOO^{\cdot}$, which are responsible for the degradation of organic dyes because of their strong oxidizing power [44].

4. Conclusion

The first part of this work concerns mainly the development and physicochemical characterization of a nanocomposite, ZnO/x% curcumin (with x =3, 5, 7, 10 and 20), where curcumin (a natural dye) is incorporated, by the wet impregnation method on the surface of ZnO nanoparticles, to improve its photocatalytic performance due to the absorption characteristics of curcumin in the visible region.

The FTIR spectroscopy results clearly show that above 10 wt.% curcumin, the characteristic peaks of curcumin appear in the FTIR spectra of the nanocomposite materials, thus indicating the formation of a separate phase of curcumin in the nanocomposite. For the ZnO/x%curcumin nanocomposite samples having a curcumin percentage below 10 wt.%, i.e. x =3, 5 and 7, no

curcumin peak is observed in the FT-IR spectra. This may be due to the low quantity of curcumin added compared to that of ZnO into the nanocomposite, which suggests that the structure of nanocomposite is imposed by that of ZnO.

In agreement with FT-IR spectram the XRD patterns of the ZnO/x%curcumin nanocomposites show that the most intense peak of pure curcumin appears only in the ZnO/20%curcumin nanocomposites. At lower curcumin percentages, the most intense peak of curcumin is absent and all of the ZnO peaks are present in all the nanocomposites.

The UV-Visible results of the nanocomposites show a shift in the maximum wavelength λ_{max} from 390 nm to 450 nm. This is due to the presence of multiple bonds and non-binding doublets, which generally allows good absorption in the visible region. Furthermore, the conjugation of electrons in the π system leads to a tightening of the π and π* levels.

In the second part of the work, we showed that it is possible to improve the photocatalytic properties of ZnO by combining it with curcumin as a photosensitizer for the elimination of an organic pollutant, Methylene Blue (MB), in aqueous solution. The photocatalytic evaluation shows a better degradation of the MB for a percentage of 5% in Curcumin, which can be considered as the optimal curcumin loading. Indeed, optimum MB degradation of 99% was obtained with 0.5 g L^{-1} nanocomposite material-catalyst dosage of 5% curcumin/ZnO, at natural pH and the initial MB concentration of 10 mg.L^{-1} for a visible light exposure of 90 min. In addition, a pseudo-first order kinetics was obtained with a rate constant (k) and half-life time ($t_{1/2}$) of 0.0423 min-1 and 16 min., respectively.

The study of the effect of the stirring parameter shows that the MB degradation rate is 19 times higher than that without stirring and the presence of air (O_2) in the solution accelerates the photocatalytic degradation of the MB dye by compared to that without air.

The significant improvement in the photocatalytic properties of ZnO, induced by the addition of curcumin as a photosensitizer under visible light irradiation, may be due to the increase in the concentration of reactive radicals species in the solution, such as superoxide ($O_2^{\cdot -}$) and hydroxyles ($OH^{\cdot}$).

Acknowledgment

The authors would like to acknowledge the Researchers Supporting Project (RSP-2024R78), King Saud University, Riyadh, Saudi Arabia.

Statements and Declarations:

Compliance with ethical standards

Conflict of interest: They have no conflict of interest

Funding

No funding

References

[1] Ling F, Fang L, Lu Y, Gao J, Wu F, Zhou M, Hu B (2016) A novel CoFe layered double hydroxides adsorbent: high adsorption amount for methyl orange dye and fast removal of Cr (VI), Microporous Mesoporous Mater 234: 230–238.

[2] Derakhshan Z, Baghapour MA, Ranjbar M, Faramarzian M,(2013) Adsorption of methylene blue dye from aqueous solutions by modified pumice stone: kinetics and equilibrium studies, Health Scope 2 (3) : 136–144.

[3] Rauf MA, Meetani MA, Khaleel A, Ahmed A (2010) Photocatalytic degradation of methylene blue using a mixed catalyst and product analysis by LC/MS, Chem. Eng. J. 157 : 373–378.

[4] Saruchi, Kumar V (2019) Adsorption kinetics and isotherms for the removal of rhodamine B dye and Pb+2 ions from aqueous solutions by a hybrid ion-exchanger, Arabian Journal of Chemistry 12: 316–329]

[5] Malik PK (2004) Dye removal from wastewater using activated carbon developed from sawdust: adsorption equilibrium and kinetics, Journal of Hazardous Materials 113(1):81-88.

[6] Cinelli G, Avino P, Notardonato I, Russo MV (2014) Ultrasound-vortex-assisted dispersive liquid-liquid microextraction coupled with gas chromatography with a nitrogen-phosphorus detector for simultaneous and rapid determination of organophosphorus pesticides and triazines in wine, Anal. Methods 6 (3): 782–790

[7] Senán-Salinas J, Landaburu-Aguirre J, Contreras-Martinez J, García-Calvo E (2022) Life Cycle Assessment application for emerging membrane recycling technologies: From reverse osmosis into forward osmosis, Resources, Conservation and Recycling (179): 106075

[8] Livraghi S., Votta A, Paganini MC, Giamello E (2005) The nature of paramagnetic species in nitrogen doped TiO2 active in visible light photocatalysis. Chem. Commun. 4; 498–500.

[9] Wahab R, Hwang I H, Kim YS, Musarrat J, Siddiqui MA, Seo HK, Tripathy SK, Shin HS (2011) Non hydrolytic synthesis and photo-catalytic studies of ZnO nanoparticles, Chemical Engineering Journal, 175: 450-457.

[10] Suwanboon S, Amornpitoksuk P, Sukolrat A (2011) Dependence of optical properties on doping metal, crystallite size and defect concentration of M-doped ZnO nanopowders (M = Al, Mg, Ti). Ceram Int, 37 : 1359-65.

[11] Wu Y, Ma Y, Zheng H, Ramakrishna S (2021) Piezoelectric materials for flexible and wearable electronics: A review, Materials & Design, 211 : 110164

[12] Kebir M, Boudjemaa A, Bachari K (2015) Enhancement photo-catalytic degradation of benzoic acid using the heterosystem $NiCo_2O_4$/ZnO, Materials Science in Semiconductor Processing, 39 : 300-307.

[13] Kao LH, Chuang KS, Catherine HN, Huang JH, Hsu HJ, Shen YC, Hu C (2023) MoS_2-coupled coniferous ZnO for photocatalytic degradation of dyes, Journal of the Taiwan Institute of Chemical Engineers, 142 :104638.

[14] Ujjan ZA, Bhatti MA, Shah AA, Tahira A, Shaikh NM, Kumar S, Mugheri AQ, Medany SS, Nafady A, Alnjiman F, Emo M, Vigolo B (2022) Simultaneous doping of sulfur and chloride ions into ZnO nanorods for improved photocatalytic properties towards degradation of methylene blue, Ceramics International 48(4) : 5535-5545.

[15] Vallejo W, Cantillo A, Salazar B, Diaz-Uribe C, Ramos W, Romero Z, Hurtado M (2020) Comparative study of ZnO thin films doped with transition metals (Cu and Co) for methylene blue photodegradation under visible irradiation, Catalysts 10 (5): 528.

[16] Bassaid S, Ziane B, Badaoui M, Chaib M, Robert D (2013) Effect of calcium oxalate on the photocatalytic degradation of Orange II on ZnO surface, Appl Nanosci 3:211–215.

[17] Swarnakar AK, Sahare S, Chander N, Gangwar RK, Bhoraskar SV, Bhave TM (2015) Nanocrystalline titanium dioxide sensitised with natural dyes for eco-friendly solar cell application, Journal of Experimental Nanoscience 10(13): 1001-1011 .

[18] Abou-Gamra Z M, Ahmed M A (2016) Synthesis of mesoporous TiO2–curcumin nanoparticles for photocatalytic degradation of methylene blue dye. Journal of Photochemistry and Photobiology B: Biology. 160 : 134-141.

[19] Krishnan S, Shriwastav A (2020) Application of TiO2 Nanoparticles Sensitized with Natural Chlorophyll Pigments as Catalyst for Visible Light Photocatalytic Degradation of Methylene Blue, Journal of Envirnmental Chemical Engineering 9(1) : 104699.

[20] Bouazza A, Bassaid S, Dehbi A, Guarnaccio A, D'Auria M (2023) Synthesis and characterization of TiO2–x% curcumin nanocomposites (with x=3, 5, and 10): application to the photocatalytic degradation of methylene blue, Reaction Kinetics, Mechanisms and Catalysis, 136 : 1589 – 1605.

[21] Bouazza A, Bassaid S, Dehbi A, Hadj-Zoubir N, Alsalme A, Robert D (2023) Use of TiO2/curcumin nanocomposite material deposited on a cellulosic film for methylene blue photocatalytic degradation under UV light, Reaction Kinetics, Mechanisms and Catalysis, 136 ; 1625 – 1641.

[22] Parra MR, Haque FZ (2014) Aqueous chemical route synthesis and the effect of calcination temperature on the structural and optical properties of ZnO nanoparticles Department of Physics, Optical Nanomaterials Lab, M.A.N.I.T., Bhopal, India, ELSEVIER, jmr&t.2014.07.001.

[23] J. Gong, W. Pu, C. Yang, J. Zhang, Tungsten and nitrogen co-doped TiO2 electrode sensitized with Fe-chlorophyllin for visible light photoelectrocatalysis, Chem. Eng. J. 209 (2012) 94–101

[24] Yallapu MM, Jaggi M, Chauhan S C (2010) β-Cyclodextrin-curcumin self-assembly enhances curcumin delivery in prostate cancer cells. Colloids Surf. B. 79: 113–125.

[25] Sanphui P, Goud N R, Khandavilli U B, Bhanoth S, Nangia A (2011) New polymorphs of curcumin, Chemical Communications (Cambridge, England) 47 (17): 5013–5015.

[26] Kakran M, Sahoo N, Tan I L, Li L (2012) Preparation of nanoparticles of poorly watersoluble antioxidant curcumin by antisolvent precipitation methods, J. Nanopart. Res. 14: 1–11.

[27] Thorat A A, Dalvi S V (2015) Solid-state phase transformations and storage stability of curcumin polymorphs, Cryst. Growth Des. 15 : 1757–1770.

[28] Homayouni A, Sadeghi F, Nokhodchi A, Varshosaz J, Garekani H A (2015) Preparation and characterization of celecoxib dispersions in soluplus®: comparison of spray drying and conventional methods, Iran. J. Pharm. Res. 14 : 35–50.

[29] Terife G, Wang P, Faridi N, Gogos C G (2012) Hot melt mixing and foaming of soluplus® and indomethacin, Polym. Eng. Sci. 52 : 1629–1639.

[30] Rumondor A F, Ivanisevic I, Bates S, Alonzo D, Taylor L (2009) Evaluation of drugpolymer miscibility in amorphous solid dispersion systems, Pharm. Res. 26 : 2523–2534.

[31] Wegiel LA, Zhao Y, Mauer LJ, Edgar KJ, Taylor LS (2014) Curcumin amorphous solid dispersions: the influence of intra and intermolecular bonding on physical stability, Pharm. Dev. Technol. 19 : 976–98.

[32] Khan SB, Rahman M, Alamry K (2013) An assessment of zinc oxide nanosheets asa selective adsorbent for cadmium; nanoscale research letters 8: 377.

[33] Thirugnanam T (2013) Effect of polymers (PEG on PVP) on sol –gel synthesis of microsized zinc oxide; Journal of nanomaterials Article ID 362175, 7 pages

[34] Dai, L., Sun, C., Li, R., Mao, L., Liu, F. and Gao, Y. (2017). Structural characterization, formation mechanism and stability of curcumin in a zein-lecithin composite nanoparticles manufactured by antisolvent co-precipitation. Food chemistry, 237, 1163-1171.

[35] Rouessac F, Rouessac A, Cruché D (2004) Méthodes et techniques instrumentales modernes, Analyse Chimique, 6° Edition DUNOD pages 144 – 145.

[36] Pradeep KS, Kirtee W, Ruchika K-G, Asmita P (2014) Correction: from micron to nano-curcumin by sophorolipid co-processing: highly enhanced bioavailability, fluorescence, and anti-cancer efficacy. RSC Adv 4:60334–60341.

[37] Mokhbi Y, Korichi M, Sidrouhou HM, Chaouche K (2014) Treatment Heterogeneous Photocatalysis; Factors Influencing the Photocatalytic Degradation by TiO2. Energy Procedia 50 559 – 566.

[38] Ishwarbhai RP, Sharma A, Sharma S (2021) Visible light-mediated applications of methylene blue in organic synthesis. Org. Chem. Front. 8 : 1694–1718.

[39] Gàbor L (2015) Deterministic Kinetics in Chemistry and Systems Biology The Dynamics of Complex Reaction Networks, Springer. http://www.springer.com/gp/book/9783319154817.

[40] Bassaid S, Robert D, Chaib M (2008) Use of oxalate sacrificial compound to improve the photocatalytic performance of titanium dioxide. Applied Catalysis B: Environmental, 86 : 93-97

[41] Linsebiclier Al, Lu G, Yates JT (1995) Photocatalysis on TiO2 surfaces: Principles, Mechanisms, and Selected Results. Chemical Reviews 95 : 735-758.

[42] Youssef Z, Colombeau L, Yesmurzayeva N, Baros F (2018) Dye-sensitized nanoparticles for heterogeneous photocatalysis : Cases studies with TiO2, ZnO, fullerene and graphene for water purification, Dye. Pigment. 159 : 49–71.

[43] Chowdhury P, Moreira J, Gomaa H, Ray AK (2012) Visible-solar-light-driven photocatalytic degradation of phenol with dye-sensitized TiO2 :Parametric and kinetic study, Ind. Eng. Chem. Res. 51 ; 4523–4532.

[44] Zhang X, Sun DD, Li G, Wanga Y (2008) Investigation of the roles of active oxygen species in photodegradation of azo dye AO7 in TiO2 photocatalysis illuminated by microwave electrodeless lamp J. Photochem. Photobiol A 199 (2-3) : 311-315

Tables

Table 1: Main assignments of FT-IR peaks coming from spectra related to curcumin molecule.

FT-IR assignments	**Wave number (cm^{-1})**
Stretching vibrations Ar-O-H	3510
Overlapping stretching vibrations of alkenes (C=C) and carbonyl (C=O)	1627
Benzene stretching vibrations	1598
C=O and C=C vibrations	1510
C-H olefinic bending vibrations	1426
C-O aromatic stretching vibrations	1280
Stretching vibrations C-O-C	1024

Table2: Particle sizes of pur ZnO and ZnO/x% Curcumin nanocomposite materials (with x = 3, 5, 7, 10 and 20)

Materials	***Dc* (nm)**
ZnO	14.35
ZnO/3%Curcumin	12.44
ZnO/5%Curcumin	15.25

ZnO/7%Curcumin	15.35
ZnO/10%Curcumin	15.45
ZnO/20%Curcumin	15.85

Table3: Values of rate constants (k), half-life times ($t_{1/2}$) and correlation coefficients (R^2) for MB photocatalytic degradation in the presence of pur ZnO, pur Curcumin and ZnO/x% Curcumin nanocomposite materials (with x = 3, 5, 7, 10 and 20)

Kinetic order	**Materials**	k	$t_{1/2}$ **(min)**	R^2
Zero order	ZnO	(0.0256 ± 0.0011) mol.L^{-1}.min^{-1}	143	0.9861
	Curcumin	(0.0219 ± 0.0008) mol.L^{-1}.min^{-1}	182	0.9901
First order	ZnO/3%Curcumin	(0.0286 ± 0.0044) min^{-1}	24	0.9911
	ZnO/5%Curcumin	(0.0423 ± 0.0030) min^{-1}	16	0.9966
	ZnO/7%Curcumin	(0.0193 ± 0.0050) min^{-1}	36	0.9881
	ZnO/10%Curcumin	(0.0106 ± 0.0036) min^{-1}	65	0.9958
	ZnO/20%Curcumin	(0.0079 ± 0.0041) min^{-1}	88	0.9979

Table 4: The values of rate constants (k), half-life times ($t_{1/2}$) and correlation coefficients (R^2) for the MB photocatalytic degradation in the presence of ZnO/5%Curcumin nanocomposite material**.**

	Stirring effect		Oxygen effect	
	Without stirring	With stirring	Without Oxygen	Under Oxygen
k	(308±11).10^{-4} mol.L^{-1}.min^{-1}	(423±30).10^{-4} min^{-1}	(155±25).10^{-4} min^{-1}	(423±30).10^{-4} min^{-1}
$t_{1/2}$ *(min)*	162	16	45	16
R^2	0.9999	0.9966	0.9981	0.9966
Reaction order	Zero	First	First	First
MB degradation (%)	28	99	85	99

Figure 1: FT-IR spectra of pure ZnO, pure curcumin and ZnO/x%Curcumin nanocomposite materials (with x = 3, 5, 7, 10 and 20).

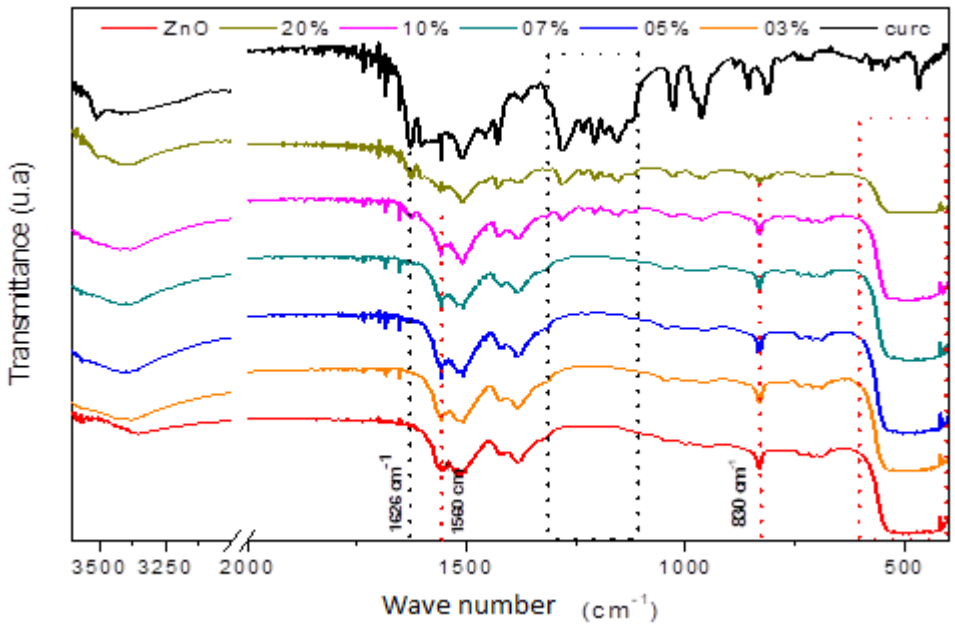

Figure 2: XRD patterns of pure ZnO, pure curcumin and ZnO/x%Curcumin nanocomposite materials (with x = 3, 5, 7, 10 and 20)

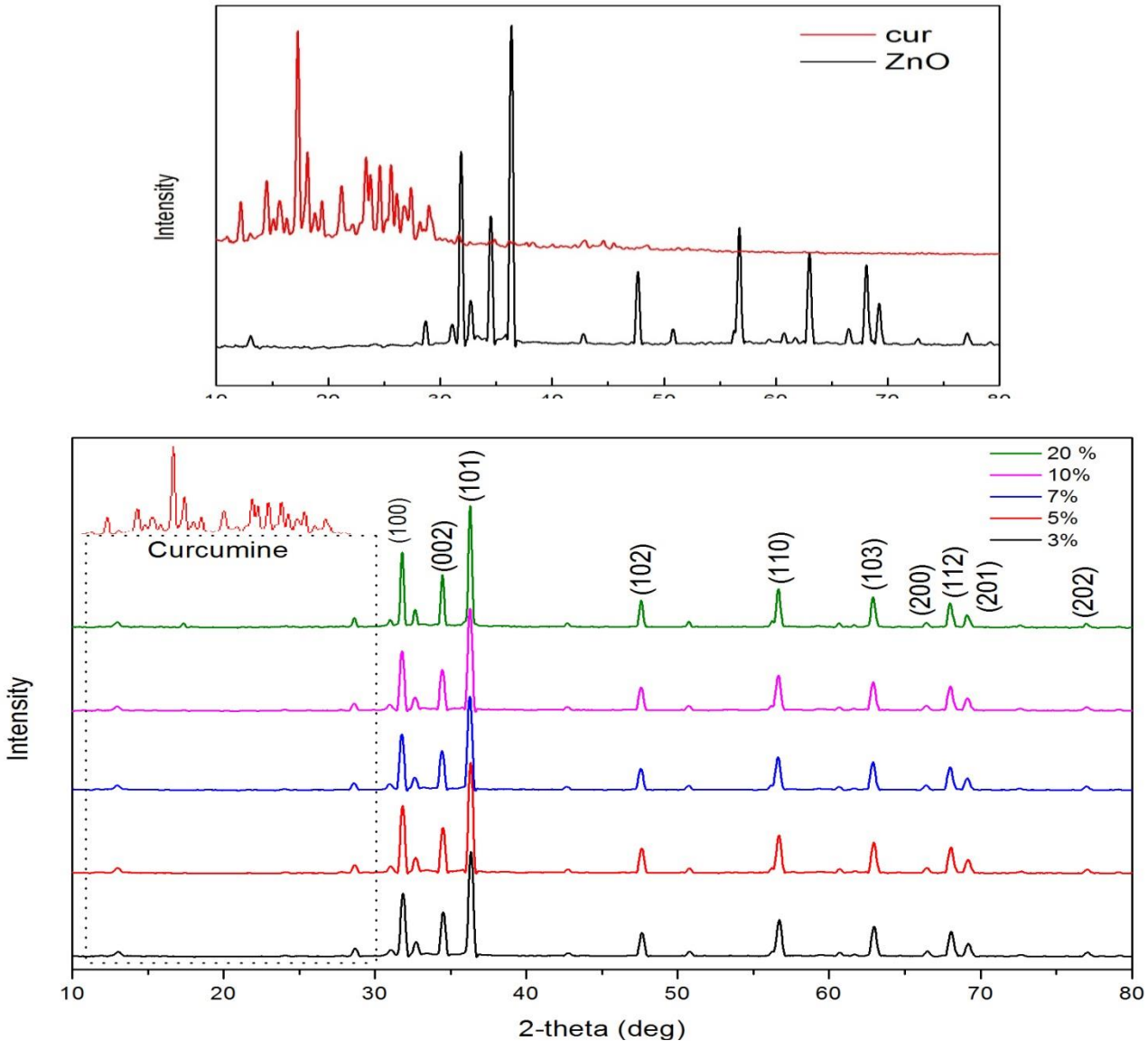

Figure 3.1 : UV-Visible spectra of pure ZnO, pure Curcumin and ZnO/x% curcumin nanocomposite materials (with x=3, 5, 7, 10 and 20)

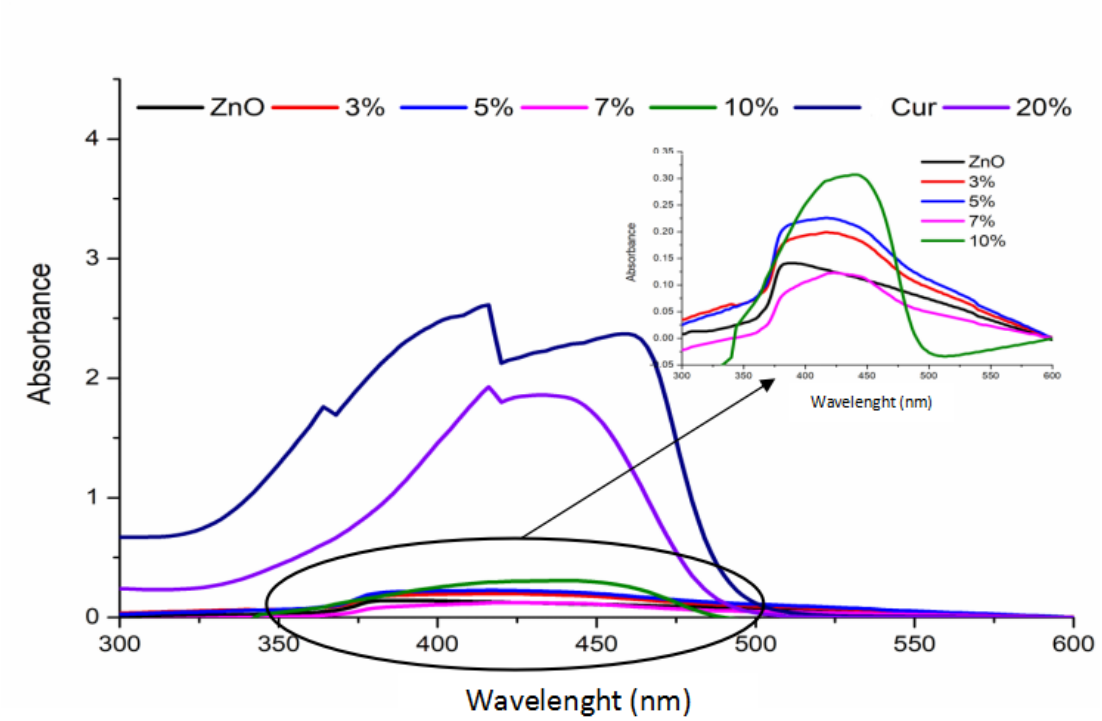

Figure 4 : SEM images of ZnO/x%Curcumin nanocomposite materials (a): Curcumin at 10.000x magnification, (b): ZnO at 30.000x magnification, (c): ZnO/5%Curcumin at 20.000x magnification, (d) : ZnO/10%Curcumin at 20.000x magnification, (e): ZnO/20%Curcumin at 20.000x magnification,

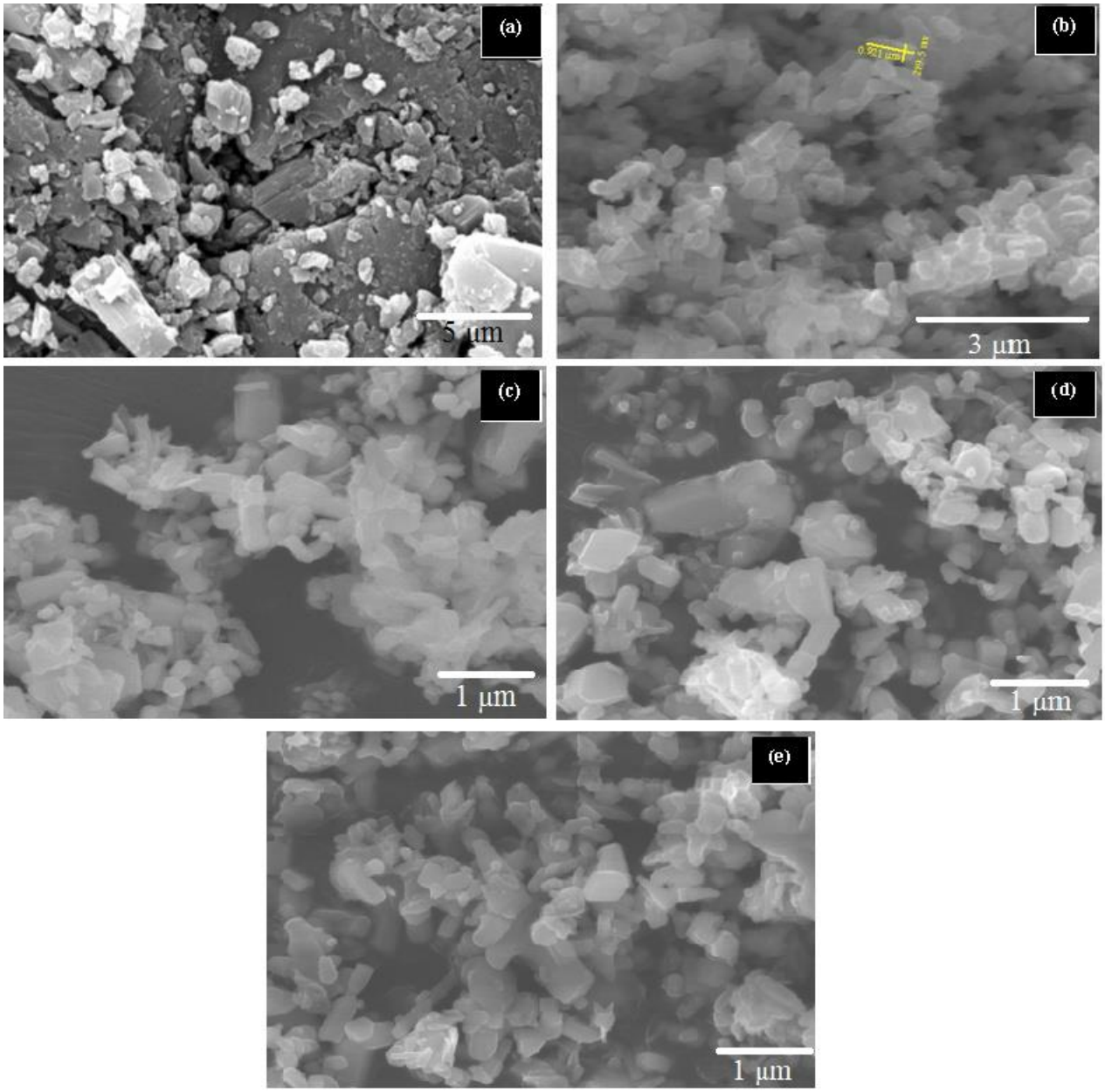

Figure 5 : Normalized concentration, C/C_0, of MB as a function of time t, under visible light irradiation in the absence of the ZnO/5%curcumin catalyst (photolysis) and in the presence of

the ZnO/5%curcumin catalyst (photocatalysis). [MB] = 10 mg.L^{-1}, 0.5 g.L^{-1} of ZnO/5%curcumin, T =25°C and at natural pH

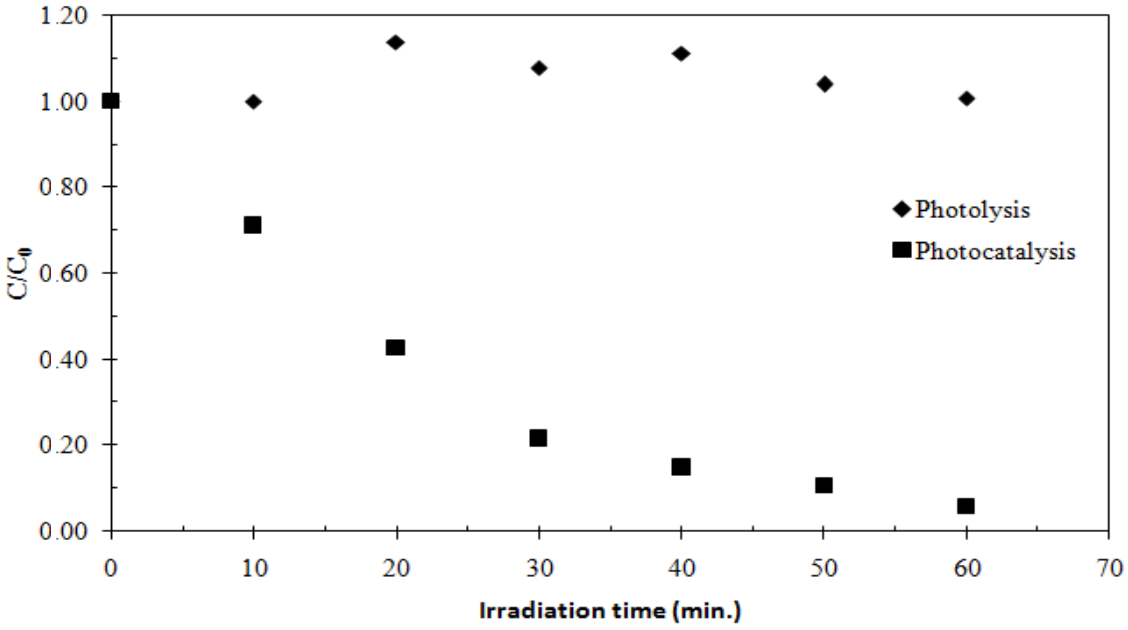

Figure 6 : MB photocatalytic degradation in the presence of pure ZnO, pure curcumin and ZnO/x%curcumin nanocomposite materials (with x = 3, 5, 7, 10 and 20) under visible light. [MB] = 10 mg.L^{-1}, 0.5 g.L^{-1} of catalyst, T =25°C and at natural pH

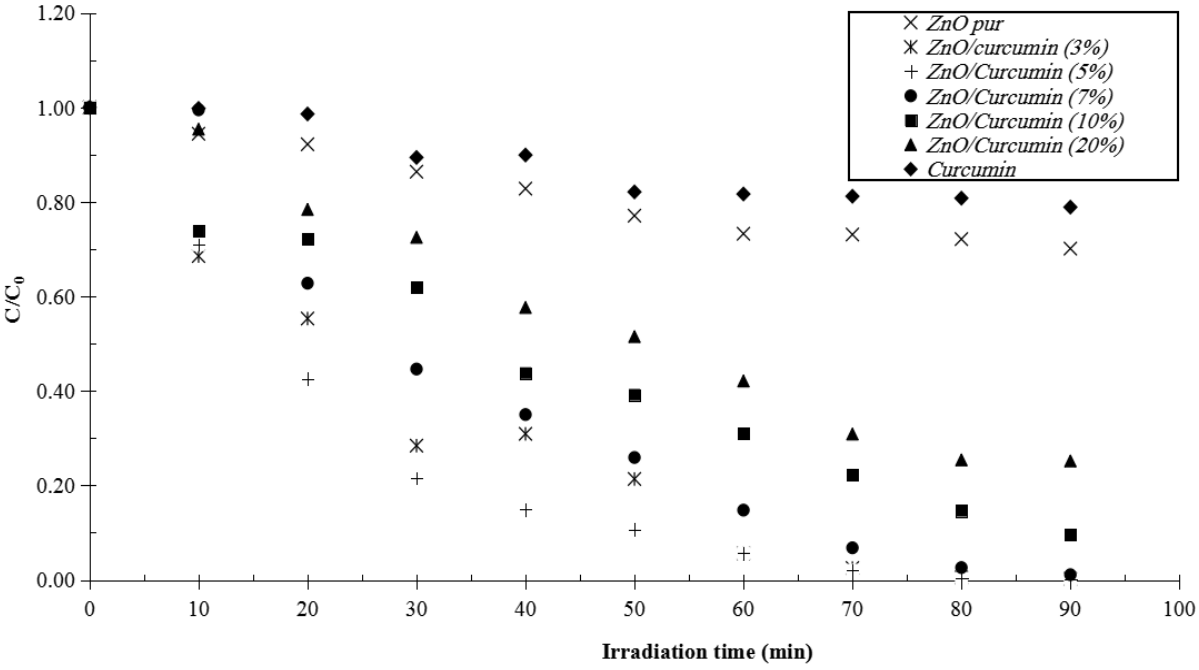
1.20
1.00
0.80
0.60
0.40
0.20
0.00
C/C0
0
10
20
30
40
50
60
70
80
90
100
Irradiation time (min)
ZnO pur
ZnO/curcumin (3%)
ZnO/Curcumin (5%)
ZnO/Curcumin (7%)
ZnO/Curcumin (10%)
ZnO/Curcumin (20%)
Curcumin

Figure 7 : Effect of stirring on MB photocatalytic degradation in presence of ZnO/5%Curcumin nanocomposite material under visible light. [MB] = 10 mg.L^{-1}, 0.5 g.L^{-1} of ZnO/5%curcumin, T =25°C and at natural pH. Stirring rate: 500 rpm

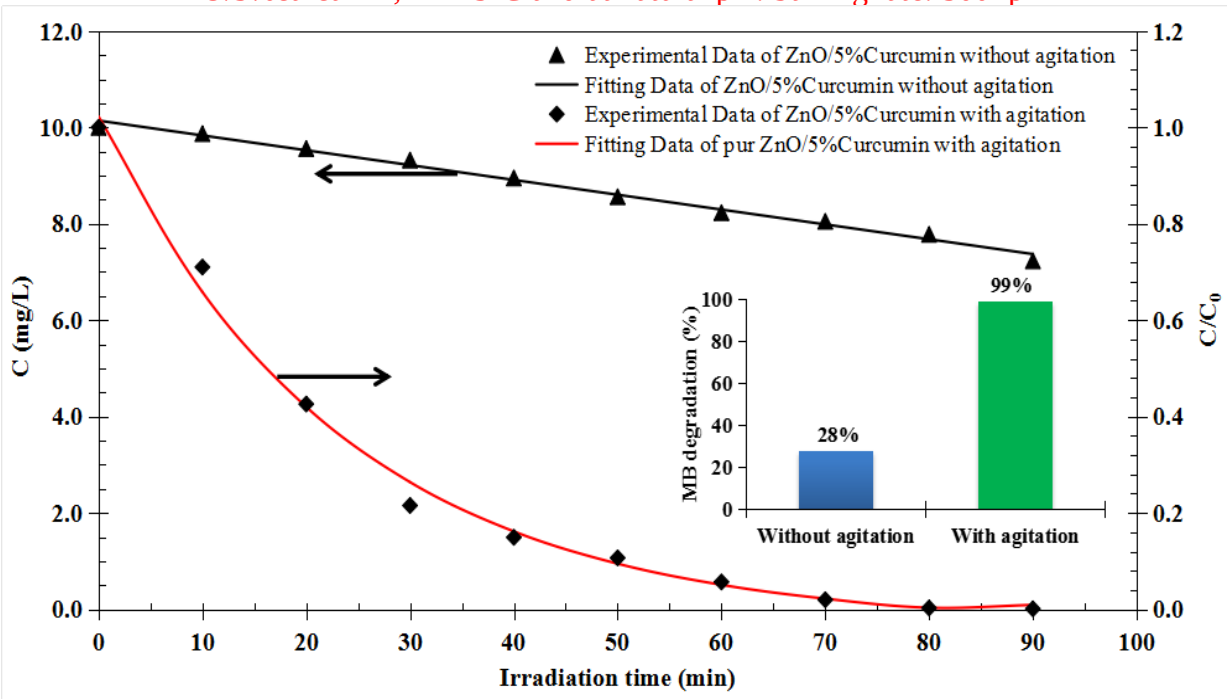

Figure 8 : Effect of oxygenation (with air) on MB photocatalytic degradation in the presence of the ZnO/5%curcumin nanocomposite material under visible light. [MB] = 10 mg.L^{-1}, 0.5 g.L^{-1} of ZnO/5%curcumin, T =25°C and at natural pH.

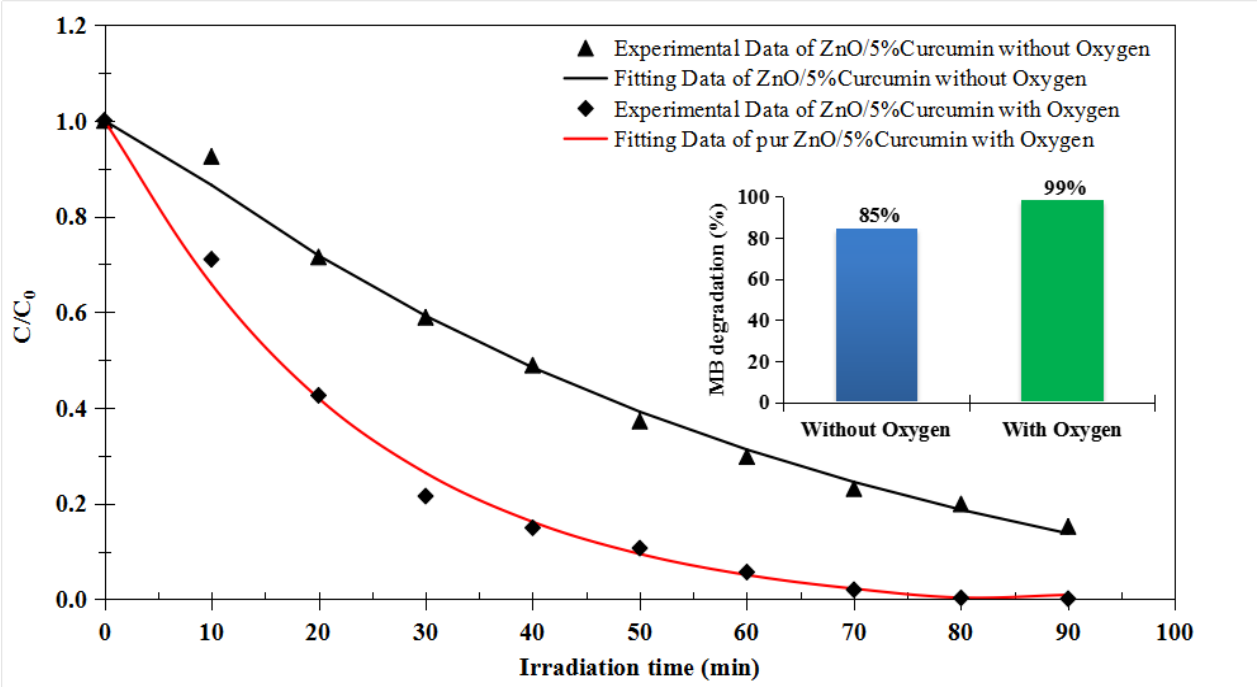
Experimental Data of ZnO/5%Curcumin without Oxygen
Fitting Data of ZnO/5%Curcumin without Oxygen
Experimental Data of ZnO/5%Curcumin with Oxygen
Fitting Data of pur ZnO/5%Curcumin with Oxygen
C/C0
Irradiation time (min)
MB degradation (%)
85%
99%
Without Oxygen
With Oxygen